

A Novel Mouse Model for Phenytoin-Induced Liver Injury: Involvement of Immune-Related Factors and P450-Mediated Metabolism

Eita Sasaki,* Kentaro Matsuo,* Azumi Iida,* Koichi Tsuneyama,† Tatsuki Fukami,* Miki Nakajima,* and Tsuyoshi Yokoi*^{1,2}

*Drug Metabolism and Toxicology, Faculty of Pharmaceutical Sciences, Kanazawa University, Kanazawa 920–1192, Japan; and †Department of Diagnostic Pathology, Graduate School of Medicine and Pharmaceutical Science for Research, University of Toyama, Toyama 930-0194, Japan

¹Present address: Department of Drug Safety Sciences Nagoya University Graduate School of Medicine, Nagoya, 466-8550, Japan

²To whom correspondence should be addressed at Department of Drug Safety Sciences Nagoya University Graduate School of Medicine 65 Tsurumai-cho, Showa-ku, Nagoya, 466-8550, Japan. Fax: +81-76-234-4407. E-mail: tyokoi@p.kanazawa-u.ac.jp.

Received May 19, 2013; accepted August 19, 2013

Drug-induced liver injury is an important issue for drug development and clinical drug therapy; however, in most cases, it is difficult to predict or prevent these reactions due to a lack of suitable animal models and the unknown mechanisms of action. Phenytoin (DPH) is an anticonvulsant drug that is widely used for the treatment of epilepsy. Some patients who are administered DPH will suffer symptoms of drug-induced liver injury characterized by hepatic necrosis. DPH-induced liver injury occurs in 1 in 1000 or 1 in 10 000 patients. Clinically, 75% of patients who develop liver injury develop a fever and 63% develop a rash. In this study, we established a mouse model for DPH-induced liver injury and analyzed the mechanisms for hepatotoxicity in the presence of immune-related or inflammation-related factors and metabolic activation. Female C57BL/6 mice were administered DPH for 5 days in combination with L-buthionine-S,R-sulfoximine. Then, the plasma alanine aminotransferase (ALT) levels were increased, hepatic lesions were observed during the histological evaluations, the hepatic glutathione levels were significantly reduced, and the oxidative stress marker levels were significantly increased. The inhibition of cytochrome P450-dependent oxidative metabolism significantly suppressed the elevated plasma ALT levels and depleted hepatic glutathione. Among the innate immune factors, the hepatic mRNA levels of NACHT, LRR, pyrin domain-containing protein 3, interleukin-1 β , and damage-associated molecular patterns were significantly increased. Prostaglandin E₁ treatment ameliorated the hepatic injury caused by DPH. In conclusion, cytochrome P450-dependent metabolic activation followed by the stimulation of the innate immune responses is involved in DPH-induced liver injury.

Key Words: phenytoin; IL-17; hepatotoxicity; glutathione; mouse model.

Drug-induced liver injury is a serious issue for new drug candidates and for products currently on the market. Phenytoin (5,5-diphenylhydantoin, DPH) is an anticonvulsant drug that is widely used for the treatment of epilepsy. A fraction of patients

administered DPH will suffer symptoms of drug hypersensitivity, typically characterized by a rash, lymphadenopathy, fever, and if the drug continues to be used, drug-induced liver injury (Dhar *et al.*, 1974; Haruda, 1979; Taylor *et al.*, 1984). Hepatic necrosis with a prominent inflammatory response occurs 1–8 weeks after exposure in between 1 in 1000 and 1 in 10 000 patients who receive DPH (Mullick and Ishak, 1980). Therefore, DPH-induced liver injury is generally recognized as idiosyncratic.

Generally, reactive metabolite formation followed by covalent binding may be associated with idiosyncratic toxicity via immune mechanisms (Spielberg *et al.*, 1981). The major metabolic pathway of DPH has been well documented. DPH is hydroxylated by cytochrome P450 (CYP) enzymes to form its phenol metabolite, 5-(*p*-hydroxyphenyl)-5-phenylhydantoin (HPPH). HPPH can be further oxidized to form the DPH catechol (Munns *et al.*, 1997). A number of *in vitro* studies show that the DPH catechol can form protein adducts in the liver microsomes of humans and mice and that DPH catechol formation is catalyzed primarily by CYP2C19 and CYP2C9 in humans (Cuttle *et al.*, 2000) and CYP2C11 in rats (Yamazaki *et al.*, 2001). Covalent bond formation is suppressed when low molecular weight thiols such as glutathione (GSH) and cysteine are present in mice microsomes (Roy and Snodgrass, 1990). Considering these *in vitro* reports, we suspect that the CYP-produced reactive metabolite of DPH covalently binding to hepatic proteins may be responsible for DPH-induced idiosyncratic toxicity. However, there are currently no *in vivo* studies on hepatic GSH content or P450 oxidation metabolism in DPH-induced liver injury due to a lack of an appropriate animal model.

Studies have shown that DPH may generate reactive oxygen species (ROS). For example, antioxidants such as superoxide dismutase (SOD), catalase, and GSH confer protection against DPH embryopathy *in vitro* (Winn and Wells, 1995) and *in vivo* (Winn and Wells, 1999). Recently, ROS have been proposed to

play an important role in the activation of the NACHT-, LRR-, and pyrin domain-containing protein 3 (NALP3) inflammasome (Bryant and Fitzgerald, 2009; Martinon *et al.*, 2009). The NALP3 inflammasome generates mature interleukin (IL)-1 β via proteolytic pathways, and mature IL-1 β engages IL-1R-harboring cells and promotes inflammatory responses (Latz, 2010; Schroder and Tschopp, 2010).

The most frequent mechanism of drug-induced liver injury is the CYP-dependent formation of reactive metabolites that cause cell death or immune reactions that amplify tissue trauma. Necrotic cell death triggers a release of damage-associated molecular patterns (DAMPs), such as the S100 protein and high-mobility group box 1 (HMGB1), which activate innate immune cells (Bianchi, 2007; Scaffidi *et al.*, 2002). The activation of innate immune cells by DAMPs occurs through toll-like receptors (TLRs; Schwabe *et al.*, 2006). Cytokines and chemokines, followed by inflammation or the infiltration of lymphocytes to hepatocytes, are involved in immune-mediated hepatotoxicity and are predominantly secreted by immune cells such as T lymphocytes and macrophages (Kita *et al.*, 2001; Oo and Adams, 2010). Cytokine production is induced by the following transcriptional factors: T-box expressed in T cells (T-bet) induces the secretion of interferon- γ and IL-12; GATA-binding domain-3 (GATA-3) induces IL-4, IL-5, and IL-13 production; and retinoid-related orphan receptor (ROR)- γ t is indispensable for the differentiation of Th17 cells, which secrete primarily IL-17 (Kidd, 2003; Langrish *et al.*, 2005; Steinman, 2007).

A number of groups including our own have also recently applied a GSH-depleted animal model to both the evaluation of hepatotoxic potential and the analysis of hepatotoxicity in several drugs that produce reactive metabolites, such as acetaminophen (Watanabe *et al.*, 2003), ticlopidine (Shimizu *et al.*, 2011), and methimazole (Kobayashi *et al.*, 2012). In an animal system depleted of GSH by a well-known GSH synthesis inhibitor, L-buthionine-S,R-sulfoximine (BSO), the tissue GSH levels were significantly reduced without any overt toxicity (Watanabe *et al.*, 2003) or any effects on the hepatic microsomal and cytosolic enzymes responsible for drug metabolism (Drew and Miners, 1984; Watanabe *et al.*, 2003).

In this study, we successfully established a DPH-induced liver injury mouse model using wild-type mice treated with DPH and BSO for 5 days. Our data suggest that DPH metabolism by CYPs and the hepatic GSH content are both involved in DPH-induced liver injury. Furthermore, the inflammation and immune factors believed to be involved in DPH-induced liver injury were investigated.

MATERIALS AND METHODS

Chemicals. DPH, BSO, and mephenytoin were purchased from Wako Pure Chemical Industries (Osaka, Japan); 1-aminobenzotriazole (ABT) was purchased from the Tokyo Chemical Industry (Tokyo, Japan). Eritoran was kindly provided by the Eisai Co. (Tokyo, Japan). Prostaglandin E₁ (PGE₁)

was purchased from Nippon Chemiphar (Tokyo, Japan). The Fuji DRI-CHEM slides for GPT/ALT-PIII, GOT/AST-PIII, and TBIL-PIII used to measure alanine aminotransferase (ALT), aspartate aminotransferase (AST), and total bilirubin (T-Bil), respectively, were from Fujifilm (Tokyo, Japan). RNAiso was obtained from Nippon Gene (Tokyo, Japan), ReverTraAce was obtained from Toyobo (Tokyo, Japan), and random hexamers and SYBR Premix EX Taq were from Takara (Osaka, Japan). All primers were commercially synthesized at Hokkaido System Sciences (Sapporo, Japan). The monoclonal anti-mouse IL-17 antibody and the monoclonal rat IgG2a isotype used as a control were obtained from R&D Systems (Abingdon, UK). The rabbit polyclonal antibody against myeloperoxidase (MPO) was obtained from DAKO (Carpinteria, CA). The Ready-SET-GO! Mouse IL-17 ELISA Kit and the Mouse IL-1 β ELISA Kit were purchased from eBioscience (San Diego, CA). The chicken anti-HMGB1 polyclonal antibody, chicken polyclonal IgY isotype, and HMGB1 ELISA Kit II were obtained from the Sino-Test Corporation (Tokyo, Japan). The other chemicals used were of analytical or the highest commercially available grade.

DPH and BSO treatments. Female C57BL/6JmsSLC mice (8 weeks old, 16–21 g) were obtained from SLC Japan (Hamamatsu, Japan). The mice were housed in a controlled environment at 23°C \pm 1°C and 50% \pm 10% humidity and with a 12-h light/12-h dark cycle in the institution's animal facility with ad libitum access to food and water. The animals were acclimatized before being used in the experiments. In this study, female C57BL/6J mice were used because female mice showed higher sensitivity to DPH-induced liver injury than male mice (data not shown). Repeated administration of DPH orally at a dose of 100 mg/kg for 6 days caused high mortality (60% of mice were dead on days 1 through 6). We speculated that this high mortality was caused by the pharmacological effects of DPH. DPH is known to induce CYPs (CyPs) in humans (Chaudhry *et al.*, 2010; Fleishaker *et al.*, 1995) and mice (Hagemeyer *et al.*, 2010). Thus, repeated administration of DPH increased DPH metabolism, contributing to the reduction of its pharmacological effects. However, the administration of DPH at a dose of 100 mg/kg for 6 days caused high mortality on days 1 and 2 due to its pharmacological effects. This phenomenon is partially explained by the fact that on days 1 and 2, induction of hepatic CyPs by DPH did not occur or was insufficient. Thus, we thought that the dose amount of DPH on days 1 and 2 should be under 100 mg/kg to reduce mortality. Therefore, we employed a dosing regimen as follows. First, 50 mg/kg of DPH was IP injected for the first 2 days. In this step, we expected to induce the hepatic CyPs by DPH. On days 3 through 5, 100 mg/kg of DPH was orally administered. In this step, we expected that the expression of hepatic CyPs had been induced by 50 mg/kg of DPH during the first 2 days of IP administration. In this dosing regimen, the mortality rate was 10%–20% on days 1 through 5. Thus, the dosage of DPH was increased to 100 mg/kg on days 3 through 5. BSO is generally administered IP. To avoid unexpected adverse interactions between DPH and BSO, we changed the dosing route of DPH on days 3 through 5. Finally, in this study, the mice were IP administered DPH in corn oil at a dose of 50 mg/kg for 2 days followed by oral administration of 100 mg/kg on days 3 through 5. BSO in saline was IP injected at a dose of 700 mg/kg 1 h prior to each DPH administration as reported by Shimizu *et al.* (2011). As a control, mice were injected with corn oil or saline, which were used as the vehicles for DPH and BSO, respectively. To determine the time-dependent changes in the plasma ALT levels, the mice were anesthetized with ether, and then blood was collected at 0 and 6 h after DPH administration on days 1 through 4 and 0, 3, 6, 24, and 48 h after the final DPH administration. Each group included 4–6 mice. At 72 h after the final DPH administration (final time point for blood collection), the blood samples were collected from the inferior vena cava for biochemical analyses. For measurement of the hepatic mRNA expression of immune- and inflammation-related factors, hepatic GSH content, protein carbonyl content, and histopathological analysis, individual mice were investigated at 24 h before (–24) and at 0, 1.5, 3, 6, 12, or 24 h after the final DPH administration. The blood samples were collected from the inferior vena cava for measurement of plasma cytokine levels. A portion of the hepatic left lobe was excised and fixed in 10% neutral buffered formalin for the histopathological examinations. The remaining liver was frozen in liquid nitrogen and stored at –80°C until use for the measurement of mRNA

expression levels, protein carbonyl content, and GSH content. Each treatment group included 3–5 mice in each time point. As a negative control, we chose mephenytoin as a structural homologue of DPH and with similar pharmacological effects to DPH. In addition, mephenytoin-induced liver injury has a low incidence compared with DPH (Zimmerman, 1999). The mice were administered mephenytoin in corn oil using the same dosing regimen as that used for DPH and BSO. To investigate the importance of the repeated administration for developing DPH-induced liver injury, we conducted a single-administration study. To investigate whether liver injury does not occur, the mice were either IP given 50 mg/kg or 100 mg/kg DPH, or they were orally given 100 or 200 mg/kg DPH and euthanized 24 h after drug administration. BSO (700 mg/kg) was IP injected 1 h prior to DPH treatment. A portion of each excised liver was fixed in a 10% formalin neutral buffer solution and used for immunohistochemistry. The degree of liver injury was assessed by hematoxylin and eosin staining and MPO staining. The plasma ALT, AST, and T-Bil levels were measured using DRI-CHEM (Fujifilm). The animals were treated and maintained in accordance with the National Institutes of Health Guide for Animal Welfare of Japan, and the animal protocols were approved by the Institutional Animal Care and Use Committee of Kanazawa University, Japan.

Treatment with ABT. One hour prior to the final DPH treatment, the mice were IP injected with ABT (100 mg/kg in saline) according to the previous studies (Shimizu et al., 2009, 2011). The vehicle was used as a control.

GSH assay. The mouse livers were homogenized in ice-cold 5% sulfosalicylic acid and centrifuged at $8000 \times g$ for 10 min. The supernatant total GSH and glutathione disulfide (GSSG) concentration was measured as previously described (Tietze, 1969). The GSH levels were calculated from the difference between the total GSH and the GSSG concentration.

Protein carbonyl content. Increased protein carbonyls are a stable indicator of oxidative stress. The protein carbonyl content of the liver homogenate was measured using a Protein Carbonyl ELISA kit (Enzo LifeScience, New York). The assay was performed according to the manufacturer's instructions.

Real-time reverse transcription (RT)-PCR. RNA from mouse liver was isolated using RNAliso (Nippon Gene, Tokyo, Japan) according to the manufacturer's instructions. The mRNA levels of S100A8, S100A9, TLR2, TLR4, TLR9, receptor for advanced glycation end products (RAGE), NALP3, IL-1 β , IL-23 p19, IL-6, GATA-3, ROR γ t, forkhead box P3 (Foxp3), Fas, FasL, T-bet, macrophage inflammatory protein-2 (MIP-2), and monocyte chemoattractant protein-1 (MCP-1) were quantified using real-time RT-PCR. For the RT step, total RNA (10 μ g) and 150 ng of random hexamers were mixed and incubated at 70°C for 10 min. The RNA solution was added to a reaction mixture containing 100 units of ReverTra Ace, reaction buffer, and 0.5 mM deoxyribonucleotide triphosphates at a final volume of 40 μ l. The resulting reaction mixture was incubated at 30°C for 10 min, 42°C for 1 h, and heated to 98°C for 10 min to inactivate the enzyme. Real-time RT-PCR was performed using the MX3000P instrument (Stratagene, La Jolla, California). The PCR mixture contained 1 μ l of template cDNA, SYBR Premix Ex Taq solution, and 8 pmol each of forward and reverse primers. The amplified products were monitored directly by measuring the increase of the SYBR Green I (Molecular Probes, Eugene, Oregon) dye intensity. The primer sequences are shown in Table 1.

Measurement of plasma HMGB1, IL-17, and IL-1 β levels. The plasma levels of HMGB1, IL-17, and IL-1 β were measured by ELISA using the HMGB1 ELISA Kit II, a Ready-SET-GO! Mouse IL-17, and a Ready-SET-GO! Mouse IL-1 β Kit, respectively, according to the manufacturers' instructions.

Administration of a TLR4 antagonist. The mice were IV treated with eritoran, a TLR4 antagonist (50 μ g/mouse in 0.2 ml sterile saline), simultaneously with the final DPH treatment as previously described (Higuchi et al., 2012). The vehicle was used as a control.

Administration of an anti-mouse IL-17 antibody or an anti-mouse HMGB1 antibody. In the IL-17 neutralization study, as described in our previous report (Higuchi et al., 2012), the mice were IV treated with an anti-mouse IL-17 antibody (100 μ g anti-mouse IL-17 antibody in 0.2 ml sterile PBS) 3 h after the final

DPH treatment. As a control, rat IgG2a was used (100 μ g rat IgG2a in 0.2 ml sterile PBS). In the HMGB1 neutralization study, the mice were IV treated with an anti-mouse HMGB1 antibody (200 μ g anti-mouse HMGB1 antibody in 0.2 ml sterile PBS) simultaneously with the final DPH treatment. As a control, a chicken IgY isotype was used (200 μ g chicken IgY in 0.2 ml sterile PBS).

Quantification of hepatic MPO-positive cells. The infiltration of neutrophils was assessed by immunostaining for MPO. A rabbit polyclonal antibody against MPO was used for the immunohistochemical staining of liver as previously described (Higuchi et al., 2012). Three visual fields of $\times 400$ magnification (0.1 mm² each) were randomly selected from each MPO-immunostained section. The total number of MPO-positive mononuclear cells from the 3 randomly selected visual fields was compared among the specimens.

Treatment with PGE₁. Three hours after the final DPH treatment, the mice were IP given PGE₁ (at 50 μ g/mouse in 0.5 ml sterile saline) as previously described (Higuchi et al., 2012; Kobayashi et al., 2009). The vehicle was used as a control.

Statistical analysis. The data are shown as the mean \pm SEM. Statistical analyses of multiple groups were performed using a one-way ANOVA with the Dunnett's post hoc test to determine the significance of the differences between individual groups. Comparisons between 2 groups were carried out using a 2-tailed Student's *t* test. A value of *p* < .05 was considered statistically significant.

RESULTS

Development of a DPH-Induced Liver Injury in C57BL/6 Mice

DPH is widely used as an anticonvulsant drug and rarely causes hepatotoxicity with or without hypersensitivity. To study the mechanism of hepatotoxicity, we developed an animal model for DPH-induced liver injury in mice. The mice were IP given DPH at a dose of 50 mg/kg for 2 days and orally administered 100 mg/kg on days 3 through 5. BSO was given on all days. With this dosing regimen, the ALT levels were significantly increased after the final DPH treatment without a high fatality rate (Fig. 1A, mortality rate was 10%–20% on days 1 through 5). These hepatotoxic effects were observed in approximately 60% of the mice, and the others showed no or mild hepatotoxicity, resulting in large SEM values. Without BSO, the plasma ALT levels were much lower than those in the BSO-treated mice. No significant elevation of ALT levels was observed in mice treated with vehicle or BSO alone (Fig. 1A).

In a single-administration study, the female C57BL/6 mice were orally given DPH at a dose of 100 or 200 mg/kg in combination with BSO. The plasma ALT level was not affected by DPH treatment (Fig. 1B). Next, the mice were IP given DPH at a dose of 50 or 100 mg/kg in combination with BSO, resulting in no hepatotoxicity caused by DPH (Fig. 1B).

Mephenytoin, used as a negative control, did not induce hepatotoxicity under the same dosing regimen as DPH, even when combined with BSO, suggesting that the hepatotoxicity of DPH is independent of its pharmacological effects (Fig. 1C).

In the histopathological experiments, apoptosis and hepatocyte ballooning were observed at 24 h after the final DPH and BSO treatment (Fig. 1D). In addition, immunohistochemistry with an anti-MPO antibody demonstrated that a number of MPO-positive cells had infiltrated in DPH- and BSO-treated mice (Fig. 1D). The

TABLE 1.
Sequences of the Primers Used for Real-time RT-PCR Analyses

| Genes | Sequences |
|-----------------|---|
| FasL | FP AGA AGG AAC TGG CAG AAC TC |
| | RP GCG GTT CCA TAT GTG TCT TC |
| Foxp3 | FP CTA GCA GTC CAC TTC ACC AAG |
| | RP GCT GCT GAG ATG TGA CTG TC |
| Gapdh | FP AAA TGG GGT GAG GCC GGT |
| | RP ATT GCT GAC AAT CTT GAG TGA |
| GATA-3 | FP GGA GGA CTT CCC CAA GAG CA |
| | RP CAT GCT GGA AGG GTG GTG A |
| IL-1 β | FP GTT GAC GGA CCC CAA AAG AT |
| | RP CAC ACA CCA GCA GGT TAT CA |
| IL-6 | FP CCA TAG CTA CCT GGA GTA CA |
| | RP GGA AAT TGG GGT AGG AAG GA |
| IL-23 p19 | FP CCA GTG TGA AGA TGG TTG TG |
| | RP CTA GTA GGG AGG TGT GAA GT |
| MIP-2 | FP AAG TTT GCC TTG ACC CTG AAG |
| | RP ATC AGG TAC GAT CCA GGC TTC |
| MCP-1 | FP TGT CAT GCT TCT GGG CTT G |
| | RP CCT CTC TCT TGA GCT TGG TG |
| NALP3 | FP GTT GAC GGA CCC CAA AAG AT |
| | RP CAC ACA CCA GCA GGT TAT CA |
| RAGE | FP GTG CTG GTT CTT GCT CTA TG |
| | RP ATC GAC AAT TCC AGT GGC TG |
| ROR- γ t | FP ACC TCC ACT GCC AGC TGT GTG CTG TC |
| | RP TCA TTT CTG CAC TTC TGC ATG TAG ACT GTC CC |
| S100A8 | FP GAG TGT CCT CAG TTT GTG CAG |
| | RP TAG ACA TAT CCA GGG ACCCAG |
| S100A9 | FP GAT GGC CAA CAA AGC ACC TT |
| | RP CCT CAA AGC TCA GCT GAT TG |
| T-bet | FP TGC CCG AAC TAC AGT CAG GAA C |
| | RP AGT GAC CTC GCC TGG TGA AAT G |
| TLR2 | FP GAA AAG ATG TCG TTC AAG GAG |
| | RP TTG CTG AAG AGG ACT GTT ATG |
| TLR4 | FP TTC TTC TCC TGC CTG ACA CC |
| | RP CCA TGC CAT GCC TTG TCT TC |
| TLR9 | FP ATT CTC TGC CGC CCA GTT TGT C |
| | RP ACG GTT GGA GAT CAA GGA GAG G |

Abbreviations: Foxp3, forkhead box P3; FP, forward primer; GATA-3, GATA-binding domain-3; IL, interleukin; MCP-1, monocyte chemoattractant protein-1; MIP-2, macrophage inflammatory protein-2; NALP3, NACHT-, LRR-, and pyrin domain-containing protein 3; RAGE, receptor for advanced glycation end products; ROR, retinoid-related orphan receptor; RP, reverse primer; T-bet, T-box expressed in T cells; TLR, toll-like receptor.

number of MPO-positive cells was significantly increased in mice given DPH or DPH plus BSO compared with vehicle-treated mice (Fig. 1E). However, liver section of DPH-alone-treated (without BSO) mice were often observed to have mild fat droplets but no apoptotic or ballooning cells, suggesting that the hepatic lesion mainly occurred in mice given both DPH and BSO. No histopathological difference was observed between the vehicle- and BSO-treated mice. Taken together, these results indicate that a DPH-induced liver injury mouse model was established.

Changes in Hepatic GSH and Oxidative Stress Marker Levels

The depletion of hepatic GSH by BSO was expected to exacerbate DPH-induced hepatotoxicity. Therefore, we investigated

whether GSH is involved in the detoxification of DPH-induced liver injury. GSH levels were significantly decreased at all time points in mice given both DPH and BSO (Fig. 2A). In mice given only DPH, the GSH levels were significantly lower at 1.5, 3, 6, and 24 h after the final DPH treatment. These results suggest that DPH has the ability to deplete hepatic GSH, leading to the development of DPH-induced hepatotoxicity.

We measured hepatic GSSG, a biomarker of oxidative stress. Changes in hepatic GSSG levels showed a similar profile to that of GSH (Fig. 2A). The total glutathione (GSH+GSSG) levels were significantly lowered in mice treated with DPH alone and DPH and BSO together. The GSH/GSSG ratio, a biomarker of oxidative stress, was significantly lowered 1.5 h after the final DPH treatment in mice given both DPH and BSO. The hepatic protein carbonyl levels, a marker of oxidative stress, were significantly increased 6 h after the final DPH treatment in mice given both DPH and BSO but not in mice given only DPH or vehicle (Fig. 2B). These results suggest that oxidative stress is involved in DPH-induced liver injury and that GSH may have a protective role in DPH-induced liver injury.

Effect of the P450 Inhibitor

To investigate whether P450-mediated metabolism is involved in DPH-induced liver injury, mice were IP given ABT (100 mg/kg), a nonspecific inhibitor of P450, 1 h prior to the final DPH administration. In the ABT-treated mice, the elevated plasma ALT and AST levels were significantly suppressed (Fig. 3A). Treatment with ABT alone or ABT and BSO together (data not shown) did not result in any changes in the ALT or AST levels compared with the vehicle-treated mice.

To confirm the involvement of reactive intermediates in the DPH-induced liver injury, we measured the effects of ABT on the hepatic GSH and GSSG levels. The hepatic GSH depletion caused by DPH was significantly restored by ABT 24 h after the final DPH treatment (Fig. 3B). ABT alone did not change the GSH levels, suggesting that ABT itself does not affect the hepatic GSH levels at this dosing regimen. The hepatic total glutathione (GSH + GSSG) levels had a similar profile to that of GSH, suggesting that GSH may be consumed by P450-mediated reactive metabolites (Fig. 3B). These results suggest that P450-mediated metabolism is involved in DPH-induced liver injury.

Changes in the Expression Levels of DAMP-Related Factors

To investigate whether DAMPs and their receptors are involved in the onset of liver injury, time-dependent changes in the hepatic mRNA expression levels of TLR9, TLR4, TLR2, S100A9, S100A8, and RAGE were measured (Fig. 4A). The mRNA expression level of TLR2 was extremely variable in the treated mice, but it was significantly increased at some time points in response to either DPH or DPH plus BSO. The expression level of S100A8 mRNA was significantly increased

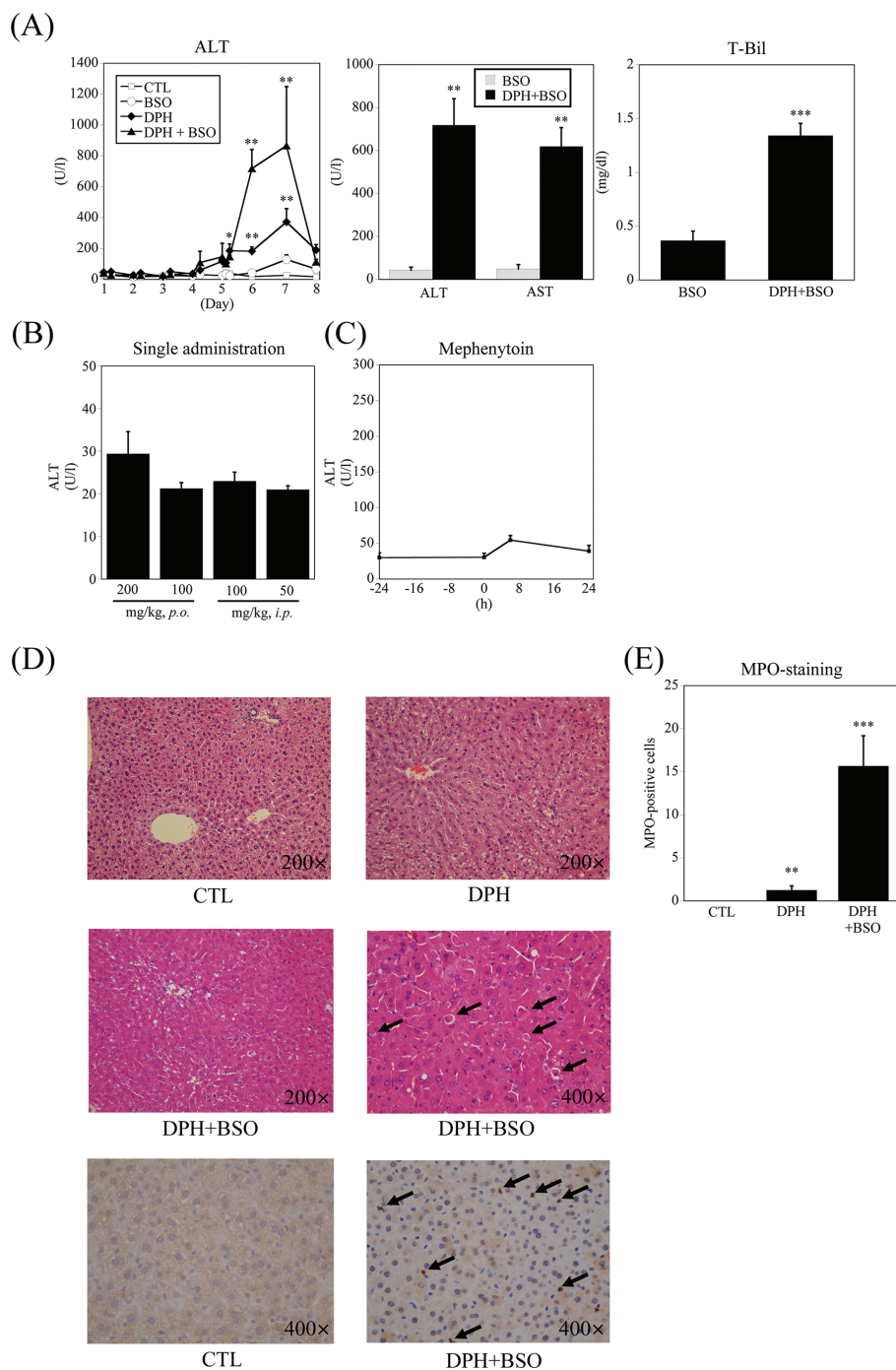


FIG. 1. Time-dependent changes in plasma ALT and AST levels in DPH-induced liver injury. A, Female C57BL/6 mice were IP given DPH at 50 mg/kg for 2 days followed by oral administration of 100 mg/kg DPH on days 3 through 5. BSO (700 mg/kg) was IP injected 1 h prior to each DPH administration. Each vehicle was used as a control. At 0 and 6 h after DPH administration on days 1–4 and at 0, 3, 6, 24, 48, and 72 h after the final DPH treatment, blood was collected to measure the plasma ALT levels. The days 6, 7, and 8 correspond to 24, 48, and 72 h after the final DPH treatment. In the second panel, the plasma ALT, AST, and T-Bil levels were measured 24 h after the final DPH treatment. The values represent the mean \pm SEM of 4–6 animals. B, In a single-administration experiment, the mice were given an oral dose of DPH at 200 or 100 mg/kg and an IP injection of 100 or 50 mg/kg. BSO (700 mg/kg) was IP injected 1 h prior to the DPH treatment, and blood was collected 24 h after DPH administration. The values represent the mean \pm SEM of 4 animals. C, As the negative control, the mice were given mephenytoin and BSO with the same dosing regimen as in (A). At 24 h before (–24) and 0, 6, and 24 h after the final mephenytoin treatment, blood was collected to measure the plasma ALT levels. Values represent the mean \pm SEM of 4 animals. D, Liver tissue sections from 24 h after the final DPH treatment were stained with hematoxylin and eosin. Neutrophil infiltration was assessed by immunostaining for MPO. The arrows indicate apoptosis or MPO-positive cells. E, The number of MPO-positive cells in mice treated with DPH and BSO, DPH alone, or vehicle. Values represent the mean \pm SEM of 4–5 specimens. The differences relative to the control mice (MPO-stained) or BSO-treated mice (ALT, AST, and T-Bil) were considered significant at $*p < .05$, $**p < .01$, and $***p < .001$. Abbreviations: ALT, alanine aminotransferase; AST, aspartate aminotransferase; BSO, L-buthionine-S,R-sulfoximine; DPH, 5,5-diphenylhydantoin; T-Bil, total bilirubin.

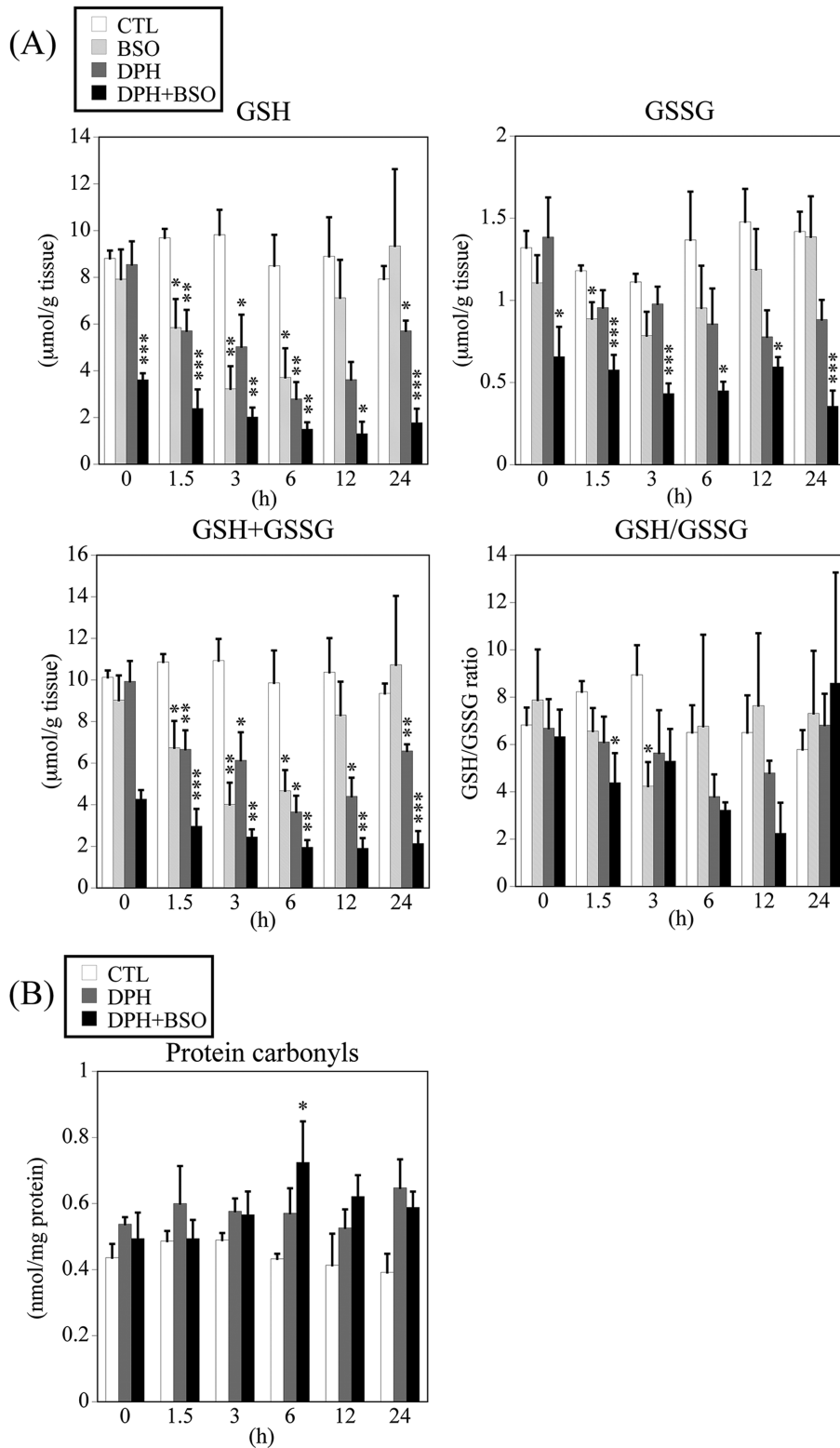


FIG. 2. Time-dependent changes in hepatic GSH, GSSG, and oxidative stress marker in DPH-induced liver injury. The mice were IP given DPH at 50 mg/kg for 2 days, and afterwards on days 3 through 5, DPH was orally administered at 100 mg/kg. BSO was IP injected 1 h prior to each DPH administration. Each vehicle was used as a control. At 0, 1.5, 3, 6, 12, and 24 h after the final DPH treatment, the liver was collected to measure the hepatic GSH, GSSG, and GSH + GSSG levels, the GSH/GSSG ratio (A), and the level of hepatic protein carbonyls (B). The data are shown as the mean \pm SEM of the results from 4 to 5 mice. The differences relative to the control mice were considered significant at * $p < .05$, ** $p < .01$, and *** $p < .001$. Abbreviations: DPH, 5,5-diphenylhydantoin; GSH, glutathione; GSSG, glutathione disulfide.

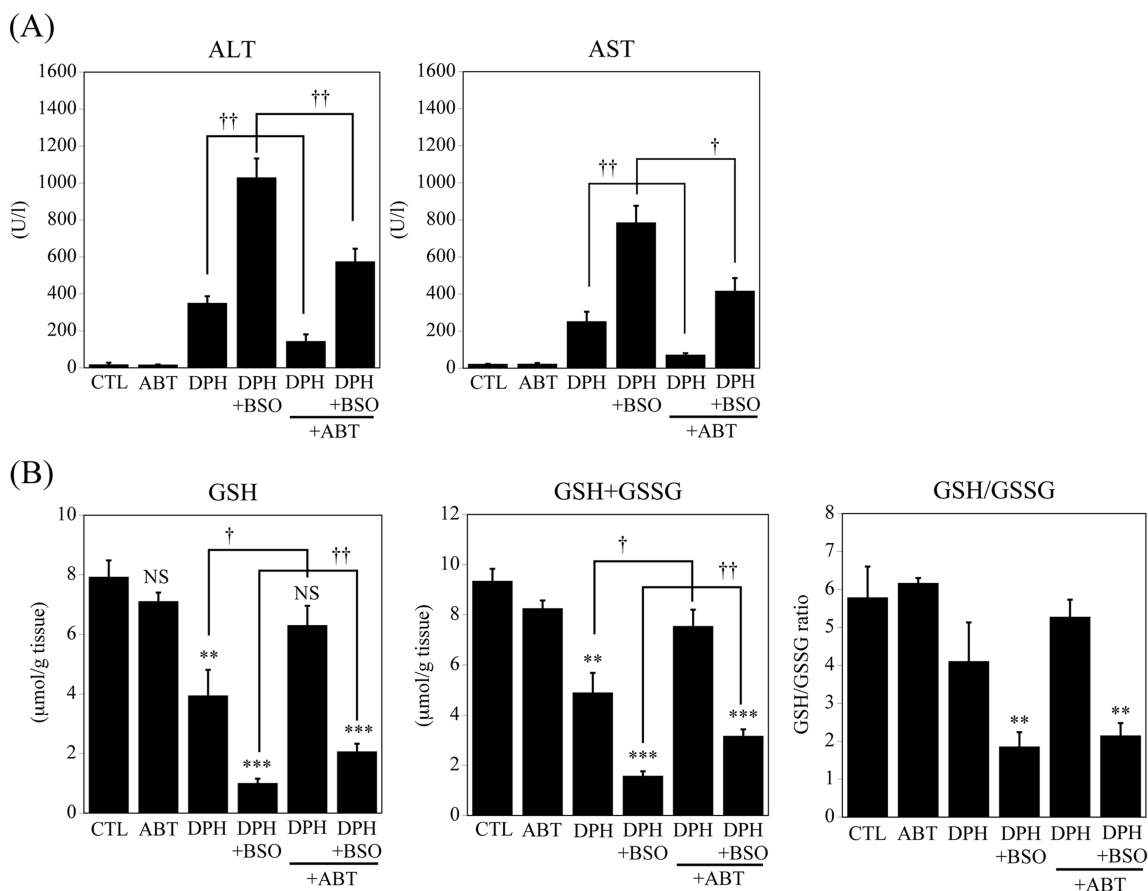


FIG. 3. Effect of a P450 inhibitor on plasma ALT and AST and hepatic GSH and GSSG levels in DPH-induced liver injury. The mice were IP given DPH at 50 mg/kg for 2 days, and then they were orally administered 100 mg/kg DPH on days 3 through 5. BSO was IP injected 1 h prior to each DPH treatment. ABT (100 mg/kg), a nonspecific inhibitor of P450, was IP given 1 h prior to the final DPH treatment. Each vehicle was used as a control. At 24 h after the final DPH treatment, the liver and plasma were collected to measure plasma ALT and AST levels (A), hepatic GSH and GSH + GSSG levels, and the GSH/GSSG ratio (B). The data are shown as the mean \pm SEM of the results from 4 mice. The differences relative to the control mice were considered significant at * $p < .05$, ** $p < .01$, and *** $p < .001$, and the differences between the ABT-treated and vehicle-treated mice were considered significant at † $p < .05$, †† $p < .01$. Abbreviations: ABT, 1-aminobenzotriazole; ALT, alanine aminotransferase; AST, aspartate aminotransferase; DPH, 5,5-diphenylhydantoin; GSH, glutathione; GSSG, glutathione disulfide; NS, not significant.

at 1.5 h, and the expression level of S100A9 was significantly increased at 12 h after the final DPH treatment. To investigate whether HMGB1 is involved in the onset of inflammation, the plasma concentration of the HMGB1 protein was measured. HMGB1 is secreted from activated immune cells and is also released from necrotic cells. Therefore, we measured plasma HMGB1 protein levels using an ELISA and observed that they were significantly increased 3 h after the final DPH treatment in mice given both DPH and BSO (Fig. 4B). These results suggest that DAMPs are involved in the onset of inflammation.

To investigate whether TLR4 signaling and HMGB1 are involved in DPH-induced liver injury, eritoran, a specific TLR4 antagonist, or an anti-HMGB1 antibody was used. Treatment with either eritoran or the anti-HMGB1 antibody significantly suppressed the elevation of plasma ALT levels, suggesting that HMGB1 and TLR4 signaling may be involved in DPH-induced liver injury (Figs. 4C and D).

Changes in the Expression Levels of NALP3 Inflammasome-Related Factors

To investigate whether the NALP3 inflammasome is involved in the onset of inflammation, time-dependent changes in the hepatic mRNA expression levels of NALP3 and IL-1 β were measured (Fig. 5A). The mRNA expression levels of IL-1 β and NALP3 were significantly increased 1.5 h after the final DPH treatment. We then investigated whether the plasma concentration of the IL-1 β protein is related to the onset of inflammation. The plasma IL-1 β protein level was significantly increased 3 h after the final DPH treatment (Fig. 5B). These results suggest that NALP3 inflammasome activation leading to IL-1 β production is involved in the onset of inflammation.

Changes in the Expression Levels of Th Cell-Related Transcription Factors, Cytokines, and Chemokines

To investigate whether inflammatory factors are involved in DPH-induced liver injury, we measured the time-dependent

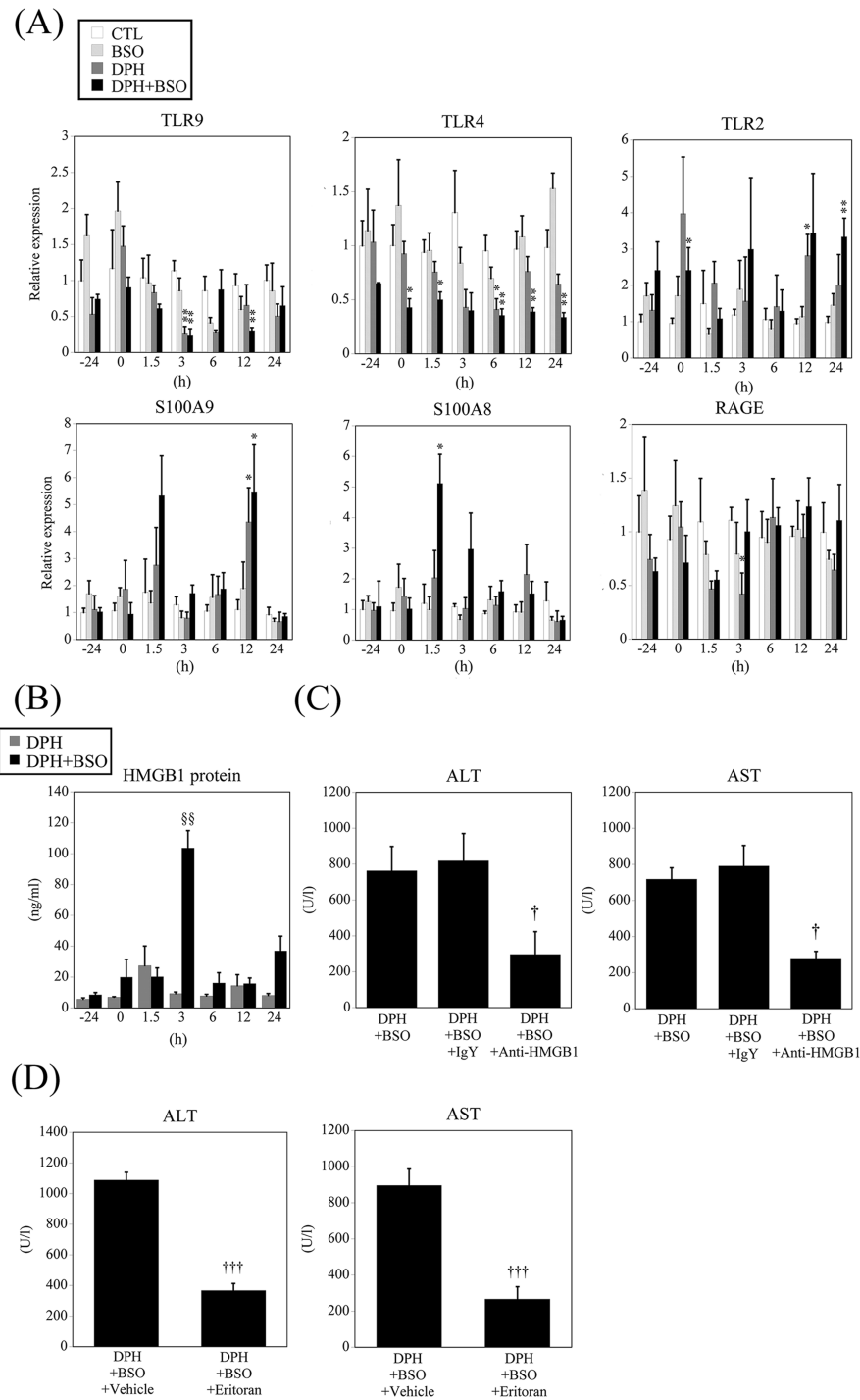


FIG. 4. Time-dependent changes in the hepatic mRNA expression levels of DAMP-related genes and plasma HMGB1 protein levels and the results of the neutralization studies in DPH-induced liver injury. A and B, Mice were IP given DPH at 50 mg/kg for 2 days, followed by oral administration of 100 mg/kg of DPH on days 3 through 5. BSO was IP injected 1 h prior to each DPH administration. Each vehicle was used as a control. At 24 h before (–24) and 0, 1.5, 3, 6, 12, and 24 h after the final DPH treatment, liver and plasma samples were collected to measure the expression of both the hepatic mRNAs of DAMP-related genes and the plasma HMGB1 protein. The expression levels of hepatic mRNAs were normalized to that of Gapdh. C, The effect of an anti-HMGB1 antibody. Mice were IV administered the anti-mouse HMGB1 antibody (200 µg anti-HMGB1 antibody in 0.2 ml sterile PBS) simultaneously with the final DPH treatment. Blood was collected 24 h after the final DPH treatment. D, The effect of eritoran, a TLR4 antagonist, on DPH-induced liver injury. Mice were IV given eritoran (50 µg/mouse in 0.2 ml sterile saline) simultaneously with the final DPH treatment. Blood was collected 24 h after the final DPH treatment. The data are shown as the mean ± SEM. The results of the time-dependent study are taken from 3 to 5 mice, and the other data are taken from 4 to 5 mice. The differences relative to the control mice were considered significant at **p* < .05, ***p* < .01, compared with the –24 h mice were considered significant at §§*p* < .01 in ELISA, and compared with isotype IgY or vehicle-treated mice were considered significant at †*p* < .05 and †††*p* < .001 in neutralization or antagonist studies, respectively. Abbreviations: BSO, L-buthionine-S,R-sulfoximine; DAMP, damage-associated molecular patterns; DPH, 5,5-diphenylhydantoin; HMGB1, high-mobility group box 1; mRNA, messenger RNA; RAGE, receptor for advanced glycation end products; TLR, toll-like receptor.

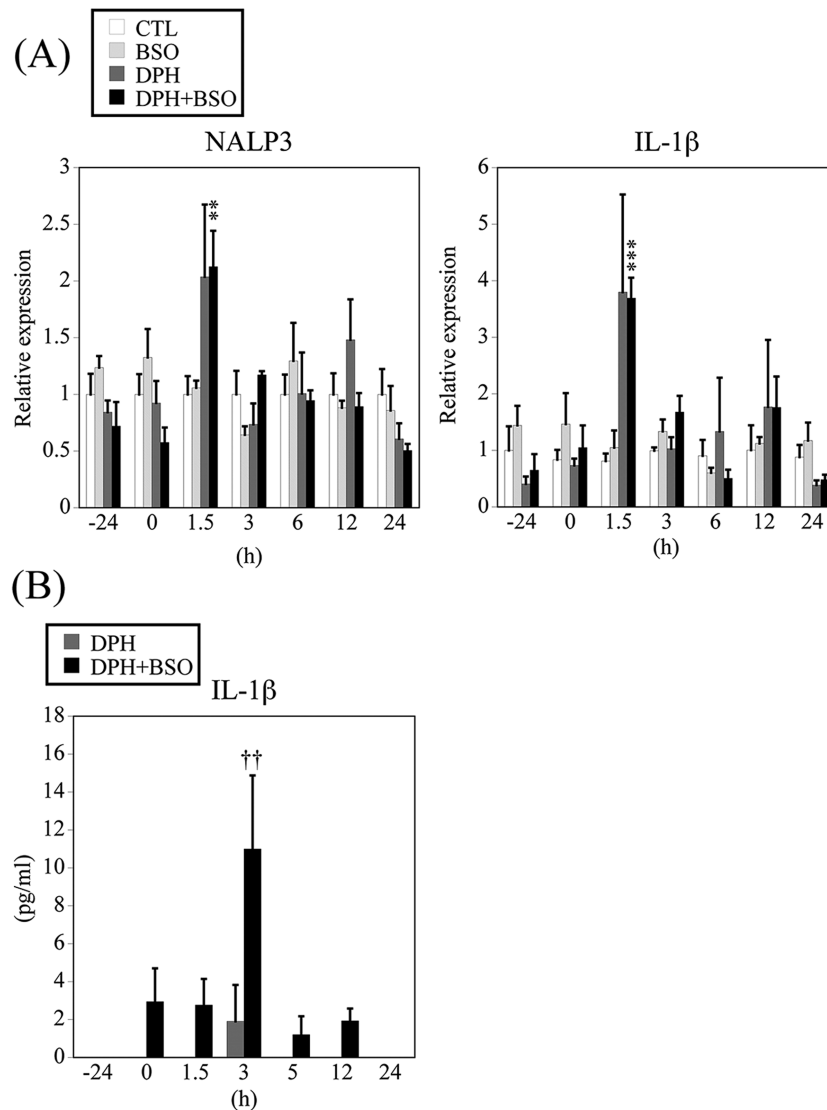


FIG. 5. Time-dependent changes in the hepatic mRNA expression levels of NALP3 and IL-1 β (A) and plasma IL-1 β protein levels (B) in DPH-induced liver injury. The experimental conditions for DPH treatments and blood and liver collection were the same as those in Figure 4. The data are shown as the mean \pm SEM of the results from 3 to 5 mice. The differences relative to the control mice were considered significant at $**p < 0.01$ and $***p < 0.001$, and the -24 h mice were considered significant at $\dagger\dagger p < 0.01$ in ELISA. Abbreviations: DPH, 5,5-diphenylhydantoin; IL, interleukin; NALP3, NACHT-, LRR-, and pyrin domain-containing protein 3; mRNA, messenger RNA.

changes in the hepatic mRNA expression levels of transcription factors for the Th lineage, cytokines, and chemokines (Fig. 6A). The hepatic mRNA expression levels of the Th17 cell-related factors IL-23 p19, IL-6, and ROR- γ t were significantly increased at some time points of measurement in mice treated with both DPH and BSO compared with the vehicle-treated mice. However, the expression levels of T-bet, GATA-3, and Foxp3, corresponding to Th1-, Th2-, and regulatory T cell-related factors, respectively, were significantly decreased in mice treated with both DPH and BSO compared with vehicle-treated mice. Following the last administration of DPH in DPH plus BSO-treated mice, the expression levels of chemokines such as MCP-1 and MIP-2 showed a time-dependent increase.

The expression levels of MIP-2 were significantly increased at 6–24 h after the last DPH administration in DPH plus BSO-treated mice compared with vehicle-treated mice. However, their levels in the mice given only BSO were not significantly altered compared with those in the mice given the vehicle. These results suggest that Th17 cell-mediated inflammation is involved in DPH-induced liver injury.

We next measured the plasma concentration of the IL-17 protein using an ELISA. A significant increase in concentration was observed at 6 h after the final DPH treatment in the mice given both DPH and BSO, whereas no significant increase was observed in the mice given only DPH (Fig. 6B). To investigate whether IL-17 was involved in DPH-induced liver injury, we

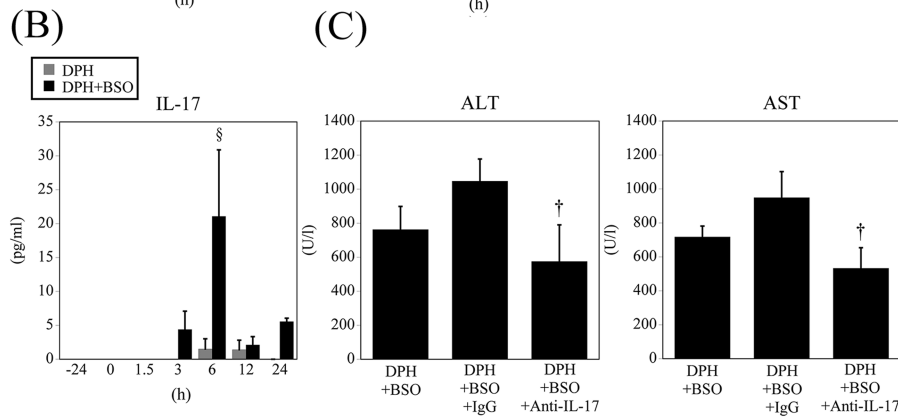
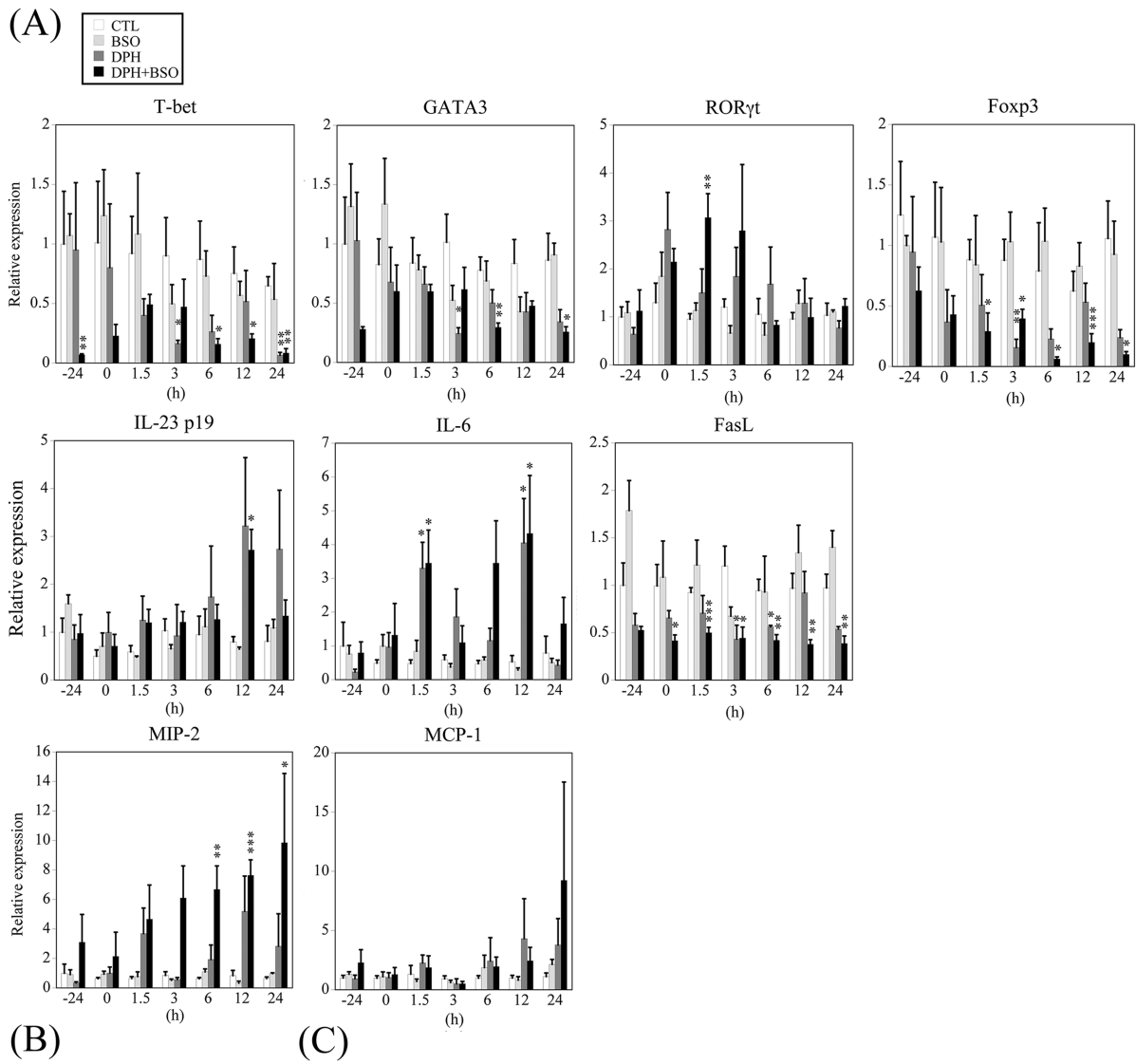


FIG. 6. Time-dependent changes in the hepatic mRNA expression levels and plasma protein levels and a neutralization study of proinflammatory cytokines and chemokines in DPH-induced liver injury. A and B, The experimental conditions for DPH treatments and blood and liver collection were the same as those in Figure 4. C, For the neutralization study, mice were IV injected with an anti-mouse IL-17 antibody (100 μg anti-mouse IL-17 antibody in 0.2 ml of sterile PBS) 3 h after the final DPH treatment. As a control, the IgG isotype was used. At 24 h after the final DPH treatment, plasma was collected to measure its ALT and AST levels. The data are shown as the mean ± SEM. The results of the time-dependent study are taken from 3 to 5 mice, and the results from the neutralization study are taken from 4 to 5 mice. The differences relative to the control mice were considered significant at **p* < .05, ***p* < .01, and ****p* < .001; -24 h mice were considered significant §*p* < .05 in ELISA; and those compared with isotype IgG-treated mice were considered significant at †*p* < .05 in neutralization study. Abbreviations: ALT, alanine aminotransferase; AST, aspartate aminotransferase; DPH, 5,5-diphenylhydantoin; IL, interleukin; mRNA, messenger RNA.

performed a neutralization study. A monoclonal anti-mouse IL-17 antibody was IV injected 3 h after the final DPH treatment. As a result, the plasma ALT and AST levels were significantly decreased 24 h after the final DPH treatment compared with the levels in mice given an isotype IgG control antibody (Fig. 6C).

The Effect of Prostaglandin E₁ on Liver Injury

PGEs are known to protect against drug-induced and immune-mediated liver injury by downregulating the production of inflammatory cytokines. To investigate the therapeutic effect of PGE₁ on DPH-induced liver injury, PGE₁ conjugated with α -cyclodextrin was IP administered to mice 3 h after the final DPH treatment according to the previously reported method (Higuchi *et al.*, 2012; Kobayashi *et al.*, 2009). The plasma ALT and AST levels were significantly decreased in mice treated with both DPH and BSO compared with the vehicle-treated mice (Fig. 7A). In addition, 24 h after the final DPH treatment (Fig. 7B), PGE₁ treatment significantly decreased the hepatic MIP-2 mRNA levels, whereas the MCP-1 mRNA levels showed a tendency to decrease compared with the vehicle-treated mice. The mRNA expression levels of IL-6 and IL-23 p19 were not significantly changed by PGE₁ (data not shown) because these mRNA expressions were not changed 24 h after the final DPH treatment. In the histopathological evaluation study, PGE₁ treatment significantly decreased the number of MPO-positive cells (Figs. 7C and D). These results suggest that PGE₁ inhibits neutrophil infiltration, likely due to the suppression of Th17 cell function.

DISCUSSION

Development of an understanding of the mechanism of drug-induced liver injury has been hampered by the lack of a suitable animal model. In this study, we first developed a model for DPH-induced liver injury in mice. In particular, we examined different conditions such as the dose of DPH, the number of doses, the dosing method, and the addition of BSO. We succeeded in developing the mouse model for DPH-induced liver injury by administering DPH at 50 mg/kg (IP, approximately one-sixth of the IP LD₅₀) DPH plus BSO for 2 days followed by a dose of 100 mg/kg (p.o., approximately one-seventh of the oral LD₅₀) plus BSO for 3 days. The mice given this treatment showed marked hepatotoxicity (Figs. 1A and D).

DPH is metabolized into an arene oxide and a catechol metabolite in human liver microsomes, suggesting that reactive metabolites are likely implicated in hepatotoxicity (Munns *et al.*, 1997). There are a number of reports showing that BSO, when given together with a drug that causes liver injury in humans, will also cause drug-induced liver injury mouse and rat models (Shimizu *et al.*, 2009, 2011) because GSH is the major antioxidant agent and is protective against toxicity by reactive metabolites or ROS. BSO is a specific

inhibitor of γ -glutamylcysteine synthetase, a rate-limiting enzyme involved in GSH synthesis, and it can decrease GSH levels *in vivo* and *in vitro* (Watanabe *et al.*, 2003). In addition, BSO was shown to have no effect on the expression levels of microsomal CYPs and phase II conjugating enzymes such as glutathione-S-transferase (GST), sulfotransferase, and uridine diphosphate-glucuronosyltransferase (Drew and Miners, 1984; Griffith and Meister, 1979; Watanabe *et al.*, 2003). Therefore, we adapted a BSO combination method to deplete hepatic GSH. In this study, BSO was administered at a dose of 700 mg/kg 1 h prior to DPH treatment as described in previous studies (Shimizu *et al.*, 2009, 2011). DPH treatment resulted in only a weak hepatotoxicity characterized by the elevation of plasma ALT levels, suggesting that GSH depletion likely exacerbates DPH-induced hepatotoxicity (Fig. 1A). These results indicate that GSH depletion is one of the risk factors for DPH-induced liver injury.

It has been reported that ROS generation is involved in drug-induced hepatotoxicity as reported in nimesulide (Ong *et al.*, 2006). Nimesulide causes mitochondrial impairment, as reflected by the decreasing mitochondrial ATP content and cytochrome C release. Therefore, we think that direct mitochondrial impairment, which is protected against by GSH, is partly involved in DPH-induced liver injury. In the histopathological analysis, apoptotic cells were observed, which might be partly caused by mitochondrial impairment (Fig. 1D).

P450 inhibitors suppressed the covalent binding of a DPH intermediate, and inducers of P450 enhanced the covalent bonding in hepatic microsomes taken from A/J mice (Roy and Snodgrass, 1990). Furthermore, GSH may modulate DPH metabolism either by trapping a DPH-reactive intermediate and decreasing the protein binding or by protecting proteins from attack by electrophilic or free radical intermediates of DPH (Roy and Snodgrass, 1990). Together, these studies and our data indicate that CYP-mediated covalent binding to hepatic proteins may be one of the mechanisms causing DPH-induced liver injury.

Administration of DPH without BSO results in a weak hepatotoxicity compared with a co-treatment with BSO, possibly due to the detoxification of reactive metabolites by GSH under normal conditions (Fig. 1A). Indeed, the administration of DPH caused significant decreases in hepatic GSH levels (Fig. 2A). The decrease in hepatic GSH content was more persistent in the mice treated with DPH plus BSO than in those treated with DPH only, and it could be that sustained reduction in GSH levels is important for toxicity.

The single administration study, even in combination with BSO, resulted in no hepatotoxicity, suggesting that the repeated administration of DPH is necessary for DPH-induced liver injury (Fig. 1B). DPH induces CYP3A4 and CYP2C9 in humans (Chaudhry *et al.*, 2010; Fleishaker *et al.*, 1995) and Cyp3a11 and Cyp2c29 in mice (Hagemeyer *et al.*, 2010), and these CYPs are involved in DPH oxidative metabolism. Therefore, the activation of DPH-inducible Cyps likely precedes

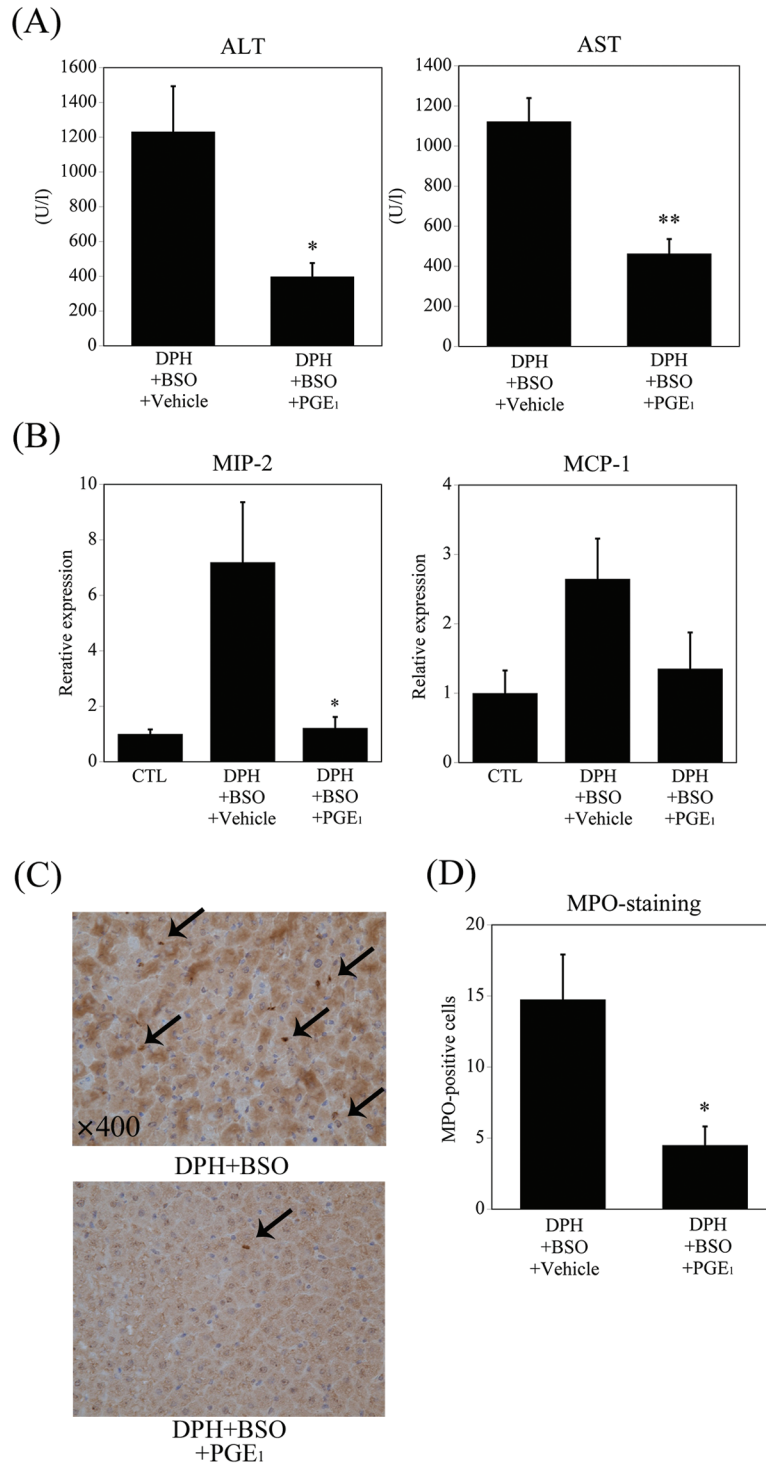


FIG. 7. Effects of PGE₁ on DPH-induced liver injury. The experimental conditions for DPH administration were the same as those in Figure 4. Mice were IP injected with PGE₁ (50 µg/mouse, dissolved in 0.5 ml sterile saline) 3h after the final DPH treatment. Each vehicle was used as a control. At 24h after the final DPH treatment, the plasma and liver were collected to measure the ALT and AST levels (A), the hepatic mRNA levels of MIP-2 and MCP-1 (B), and for immunohistochemistry (C and D). The expression level of hepatic mRNA was normalized to that of Gapdh. Mononuclear cell infiltration was assessed by immunostaining for MPO. The number of MPO-positive cells in DPH and BSO-treated or DPH, BSO, and PGE₁-treated mice is shown in (D). The arrows indicate MPO-positive cells. The data are shown as the mean ± SEM of the results from 4 to 5 mice. The differences compared with the DPH-treated, BSO-treated, and vehicle-treated mice were considered significant at **p* < .05 and ***p* < .01. Abbreviations: ALT, alanine aminotransferase; AST, aspartate aminotransferase; BSO, L-buthionine-S,R-sulfoximine; DPH, 5,5-diphenylhydantoin; MCP-1, monocyte chemoattractant protein-1; MIP-2, macrophage inflammatory protein-2; MPO, myeloperoxidase; mRNA, messenger RNA; PGE₁, Prostaglandin E₁.

the onset of DPH-induced liver injury. During repeated dosing with DPH, even with BSO, no increase in ALT levels was observed on days 1–3 (Fig. 1A). We speculate that the quantity of DPH-inducible Cyps on the fourth day is sufficient to produce the reactive metabolites required for the development of liver injury. Pretreatment with ABT, a nonspecific inhibitor of P450 that can reduce the oxidative metabolism of drugs *in vivo* without any overt toxicity (Shimizu *et al.*, 2009), on the fifth day significantly suppressed the elevation of the ALT levels and the hepatic GSH depletion by DPH plus BSO (Fig. 3A). These data also indicate that P450-mediated metabolism is involved in DPH-induced liver injury.

Previous studies on DPH-induced liver injury in humans show severe hepatocellular injury with a prominent inflammatory response and massive necrosis (Mullick and Ishak, 1980). In this study, hepatic apoptosis, ballooning cells, and neutrophil infiltration were observed in DPH-induced liver injury in mice (Fig. 1D). Necrotic or apoptotic cells trigger a release of cell contents, and as a result, some of the released endogenous compounds are able to activate innate immune cells (Scaffidi *et al.*, 2002). HMGB1 is one of the first DAMPs identified, which is released during endogenous tissue trauma. However, a large number of other molecules, including heat shock proteins, S100A8/9, DNA, RNA, and others, can also function as DAMPs (Bianchi, 2007). The activation of innate immune cells by DAMPs occurs through TLRs, which recognize various molecular patterns including one in HMGB1 (Schwabe *et al.*, 2006).

Mature IL-1 β protein is produced by cleavage of precursor IL-1 β by caspase-1. The release of active IL-1 β engages cells containing IL-1R and promotes inflammatory responses (Bryant and Fitzgerald, 2009; Latz, 2010). Therefore, we thought that IL-1 β protein levels do not reflect the mRNA expression levels of IL-1 β . Indeed, the mRNA levels of IL-1 β were similar between DPH plus BSO-treated and DPH-treated mice, whereas the plasma IL-1 β protein levels were significantly increased in DPH plus BSO-treated mice. As reviewed in Latz (2010), Schroder and Tschopp (2010), and Scaffidi *et al.*, (2002), the NALP3 inflammasome is activated by DAMPs that are released from injured cells. The NALP3 inflammasome generates mature IL-1 β via proteolytic pathways. Recently, oxidative stress has been shown to play an important role in the activation of the NALP3 inflammasome (Bryant and Fitzgerald, 2009; Martinon *et al.*, 2009; Zhou *et al.*, 2010). In this study, DPH and BSO together significantly increased an oxidative stress marker, the protein carbonyl, suggesting that DPH-generated oxidative stress may be involved in the activation of the NALP3 inflammasome (Fig. 2B).

On the basis of our results, we speculate that the secretion of DAMPs from cells that are injured by reactive metabolites or ROS results in the activation of the NALP3 inflammasome and TLR4 signaling; these processes are factors in the early onset of liver injury because their mRNA levels were increased at relatively early time points. Additionally, we showed that HMGB1 and TLR4 are involved in DPH-induced liver injury (Figs. 4B and C).

Although the mechanism of drug-induced liver injury is still unclear due to the lack of animal models, LPS (lipopolysaccharide)-treated rodent models showed high sensitivity to human hepatotoxic drugs, such as trovafloxacin (Shaw *et al.*, 2009). LPS can activate innate immune responses via TLR4, which might suggest that the susceptibility to innate immune responses is one of the risk factors of DPH-induced liver injury.

In an adaptive immune reaction, Th17 cells may be involved in some types of drug-induced liver injury (Higuchi *et al.*, 2012; Kobayashi *et al.*, 2009). IL-1 β and IL-6 or IL-1 β together with IL-23 induce Th17 cell differentiation (Acosta-Rodriguez *et al.*, 2007). IL-17, which is produced mainly by a specific subset of Th17 cells, stimulates the production of CXC chemokines such as MIP-2 and plays an important role in neutrophil activity (Langrish *et al.*, 2005; Steinman, 2007). IL-17 is involved in autoimmune responses and some immune-mediated drug-induced liver injuries in mice (Higuchi *et al.*, 2012; Kobayashi *et al.*, 2009). These findings prompted us to investigate the involvement of IL-17 in DPH-induced liver injury. The neutralization of IL-17 significantly inhibited the previously increased plasma ALT and AST levels, suggesting that IL-17 is involved in DPH-induced liver injury (Fig. 6B).

A previous study showed that PGE₁ inhibited neutrophil superoxide production (Talpain *et al.*, 1995) and had a protective effect against drug-induced liver injury in mice. For mice with halothane- and carbamazepine-induced liver injuries, PGE₁ inhibits the increased plasma ALT and IL-17 levels, as well as the expression levels of hepatic MIP-2, IL-6, and IL-23 p19, suggesting that PGE₁ has a protective effect on IL-17-mediated liver injury (Higuchi *et al.*, 2012; Kobayashi *et al.*, 2009). In this study, the elevation of plasma ALT and AST levels, hepatic MIP-2 mRNA expression levels, and the number of hepatic MPO-positive cells were significantly inhibited by PGE₁ (Figs. 7A–C). As a result, we conclude that PGE₁ may be used for pharmacotherapy in DPH-induced liver injury.

In conclusion, in this study, we first established DPH-induced liver injury in mice. We demonstrated that DPH-induced liver injury is related to hepatic GSH levels, oxidative metabolism by Cyps, the innate immune response, and Th17 cell-mediated inflammation. These observations may aid in understanding the risk factors for and the mechanism of the idiosyncratic hepatotoxicity of DPH in humans.

FUNDING

Health and Labor Sciences Research Grants from the Ministry of Health, Labor and Welfare of Japan (H24-BIO-G001).

REFERENCES

- Acosta-Rodriguez, E. V., Napolitani, G., Lanzavecchia, A., and Sallusto, F. (2007). Interleukins 1beta and 6 but not transforming growth factor-beta are essential for the differentiation of interleukin 17-producing human T helper cells. *Nat. Immunol.* **8**, 942–949.

- Bianchi, M. E. (2007). DAMPs, PAMPs and alarmins: All we need to know about danger. *J. Leukoc. Biol.* **81**, 1–5.
- Bryant, C., and Fitzgerald, K. A. (2009). Molecular mechanisms involved in inflammasome activation. *Trends Cell Biol.* **19**, 455–464.
- Chaudhry, A. S., Urban, T. J., Lamba, J. K., Birnbaum, A. K., Rimmel, R. P., Subramanian, M., Strom, S., You, J. H., Kasperaviciute, D., Catarino, C. B., et al. (2010). CYP2C9*1B promoter polymorphisms, in linkage with CYP2C19*2, affect phenytoin autoinduction of clearance and maintenance dose. *J. Pharmacol. Exp. Ther.* **332**, 599–611.
- Cuttle, L., Munns, A. J., Hogg, N. A., Scott, J. R., Hooper, W. D., Dickinson, R. G., and Gillam, E. M. (2000). Phenytoin metabolism by human cytochrome P450: involvement of P450 3A and 2C forms in secondary metabolism and drug-protein adduct formation. *Drug Metab. Dispos.* **28**, 945–950.
- Dhar, G. J., Pierach, C. A., Ahamed, P. N., and Howard, R. B. (1974). Diphenylhydantoin-induced hepatic necrosis. *Postgrad. Med.* **56**, 128–134.
- Drew, R., and Miners, J. O. (1984). The effects of buthionine sulphoximine (BSO) on glutathione depletion and xenobiotic biotransformation. *Biochem. Pharmacol.* **33**, 2989–2994.
- Fleishaker, J. C., Pearson, L. K., and Peters, G. R. (1995). Phenytoin causes a rapid increase in 6 beta-hydroxycortisol urinary excretion in humans—A putative measure of CYP3A induction. *J. Pharm. Sci.* **84**, 292–294.
- Griffith, O. W., and Meister, A. (1979). Potent and specific inhibition of glutathione synthesis by buthionine sulfoximine (S-n-butyl homocysteine sulfoximine). *J. Biol. Chem.* **254**, 7558–7560.
- Hagemeyer, C. E., Bürck, C., Schwab, R., Knoth, R., and Meyer, R. P. (2010). 7-Benzyloxyresorufin-O-dealkylase activity as a marker for measuring cytochrome P450 CYP3A induction in mouse liver. *Anal. Biochem.* **398**, 104–111.
- Haruda, F. (1979). Phenytoin hypersensitivity: 38 cases. *Neurology* **29**, 1480–1485.
- Higuchi, S., Yano, A., Takai, S., Tsuneyama, K., Fukami, T., Nakajima, M., and Yokoi, T. (2012). Metabolic activation and inflammation reactions involved in carbamazepine-induced liver injury. *Toxicol. Sci.* **130**, 4–16.
- Kidd, P. (2003). Th1/Th2 balance: The hypothesis, its limitations, and implications for health and disease. *Altern. Med. Rev.* **8**, 223–246.
- Kita, H., Mackay, I. R., Van De Water, J., and Gershwin, M. E. (2001). The lymphoid liver: Considerations on pathways to autoimmune injury. *Gastroenterology* **120**, 1485–1501.
- Kobayashi, E., Kobayashi, M., Tsuneyama, K., Fukami, T., Nakajima, M., and Yokoi, T. (2009). Halothane-induced liver injury is mediated by interleukin-17 in mice. *Toxicol. Sci.* **111**, 302–310.
- Kobayashi, M., Higuchi, S., Ide, M., Nishikawa, S., Fukami, T., Nakajima, M., and Yokoi, T. (2012). Th2 cytokine-mediated methimazole-induced acute liver injury in mice. *J. Appl. Toxicol.* **32**, 823–833.
- Langrish, C. L., Chen, Y., Blumenschein, W. M., Mattson, J., Basham, B., Sedgwick, J. D., McClanahan, T., Kastelein, R. A., and Cua, D. J. (2005). IL-23 drives a pathogenic T cell population that induces autoimmune inflammation. *J. Exp. Med.* **201**, 233–240.
- Latz, E. (2010). The inflammasomes: Mechanisms of activation and function. *Curr. Opin. Immunol.* **22**, 28–33.
- Martinon, F., Mayor, A., and Tschopp, J. (2009). The inflammasomes: Guardians of the body. *Annu. Rev. Immunol.* **27**, 229–265.
- Mullick, F. G., and Ishak, K. G. (1980). Hepatic injury associated with diphenylhydantoin therapy. A clinicopathologic study of 20 cases. *Am. J. Clin. Pathol.* **74**, 442–452.
- Munns, A. J., De Voss, J. J., Hooper, W. D., Dickinson, R. G., and Gillam, E. M. (1997). Bioactivation of phenytoin by human cytochrome P450: Characterization of the mechanism and targets of covalent adduct formation. *Chem. Res. Toxicol.* **10**, 1049–1058.
- Ong, M. M., Wang, A. S., Leow, K. Y., Khoo, Y. M., and Boelsterli, U. A. (2006). Nimesulide-induced hepatic mitochondrial injury in heterozygous Sod2(+/-) mice. *Free Radic. Biol. Med.* **40**, 420–429.
- Oo, Y. H., and Adams, D. H. (2010). The role of chemokines in the recruitment of lymphocytes to the liver. *J. Autoimmun.* **34**, 45–54.
- Roy, D., and Snodgrass, W. R. (1990). Covalent binding of phenytoin to protein and modulation of phenytoin metabolism by thiols in A/J mouse liver microsomes. *J. Pharmacol. Exp. Ther.* **252**, 895–900.
- Scaffidi, P., Misteli, T., and Bianchi, M. E. (2002). Release of chromatin protein HMGB1 by necrotic cells triggers inflammation. *Nature* **418**, 191–195.
- Schroder, K., and Tschopp, J. (2010). The inflammasomes. *Cell* **140**, 821–832.
- Schwabe, R. F., Seki, E., and Brenner, D. A. (2006). Toll-like receptor signaling in the liver. *Gastroenterology* **130**, 1886–1900.
- Shaw, P. J., Ditewig, A. C., Waring, J. F., Liguori, M. J., Blomme, E. A., Ganey, P. E., and Roth, R. A. (2009). Coexposure of mice to trovafloxacin and lipopolysaccharide, a model of idiosyncratic hepatotoxicity, results in a unique gene expression profile and interferon gamma-dependent liver injury. *Toxicol. Sci.* **107**, 270–280.
- Shimizu, S., Atsumi, R., Itokawa, K., Iwasaki, M., Aoki, T., Ono, C., Izumi, T., Sudo, K., and Okazaki, O. (2009). Metabolism-dependent hepatotoxicity of amodiaquine in glutathione-depleted mice. *Arch. Toxicol.* **83**, 701–707.
- Shimizu, S., Atsumi, R., Nakazawa, T., Izumi, T., Sudo, K., Okazaki, O., and Saji, H. (2011). Ticlopidine-induced hepatotoxicity in a GSH-depleted rat model. *Arch. Toxicol.* **85**, 347–353.
- Spielberg, S. P., Gordon, G. B., Blake, D. A., Goldstein, D. A., and Herlong, H. F. (1981). Predisposition to phenytoin hepatotoxicity assessed in vitro. *N. Engl. J. Med.* **305**, 722–727.
- Steinman, L. (2007). A brief history of T(H)17, the first major revision in the T(H)1/T(H)2 hypothesis of T cell-mediated tissue damage. *Nat. Med.* **13**, 139–145.
- Talpain, E., Armstrong, R. A., Coleman, R. A., and Vardey, C. J. (1995). Characterization of the PGE receptor subtype mediating inhibition of superoxide production in human neutrophils. *Br. J. Pharmacol.* **114**, 1459–1465.
- Taylor, J. W., Stein, M. N., Murphy, M. J., and Mitros, F. A. (1984). Cholestatic liver dysfunction after long-term phenytoin therapy. *Arch. Neurol.* **41**, 500–501.
- Tietze, F. (1969). Enzymic method for quantitative determination of nanogram amounts of total and oxidized glutathione: Applications to mammalian blood and other tissues. *Anal. Biochem.* **27**, 502–522.
- Watanabe, T., Sagisaka, H., Arakawa, S., Shibaya, Y., Watanabe, M., Igarashi, I., Tanaka, K., Totsuka, S., Takasaki, W., and Manabe, S. (2003). A novel model of continuous depletion of glutathione in mice treated with L-buthionine (S,R)-sulfoximine. *J. Toxicol. Sci.* **28**, 455–469.
- Winn, L. M., and Wells, P. G. (1995). Phenytoin-initiated DNA oxidation in murine embryo culture, and embryo protection by the antioxidative enzymes superoxide dismutase and catalase: Evidence for reactive oxygen species-mediated DNA oxidation in the molecular mechanism of phenytoin teratogenicity. *Mol. Pharmacol.* **48**, 112–120.
- Winn, L. M., and Wells, P. G. (1999). Maternal administration of superoxide dismutase and catalase in phenytoin teratogenicity. *Free Radic. Biol. Med.* **26**, 266–274.
- Yamazaki, H., Komatsu, T., Takemoto, K., Saeki, M., Minami, Y., Kawaguchi, Y., Shimada, N., Nakajima, M., and Yokoi, T. (2001). Decreases in phenytoin hydroxylation activities catalyzed by liver microsomal cytochrome P450 enzymes in phenytoin-treated rats. *Drug Metab. Dispos.* **29**, 427–434.
- Zhou, R., Tardivel, A., Thorens, B., Choi, I., and Tschopp, J. (2010). Thioredoxin-interacting protein links oxidative stress to inflammasome activation. *Nat. Immunol.* **11**, 136–140.
- Zimmerman, H. J. (1999). *Hepatotoxicity: The Adverse Effects of Drugs and Other Chemicals on the Liver*. Lippincott Williams & Wilkins, Philadelphia, PA.